



## SHALLOW WATER FLOW MODELING USING SPACE-TIME LEAST-SQUARES FINITE-ELEMENT METHOD

Shin-Jye Liang

*Department of Marine Environmental Informatics, National Taiwan Ocean University, Keelung, Taiwan, R.O.C.,  
sjliang@ntou.edu.tw*

Chiung-Yang Lan

*Department of Marine Environmental Informatics, National Taiwan Ocean University, Keelung, Taiwan, R.O.C.*

Ying-Chih Chen

*Department of Marine Environmental Informatics, National Taiwan Ocean University, Keelung, Taiwan, R.O.C.*

Follow this and additional works at: <https://jmstt.ntou.edu.tw/journal>



Part of the [Oceanography and Atmospheric Sciences and Meteorology Commons](#)

### Recommended Citation

Liang, Shin-Jye; Lan, Chiung-Yang; and Chen, Ying-Chih (2012) "SHALLOW WATER FLOW MODELING USING SPACE-TIME LEAST-SQUARES FINITE-ELEMENT METHOD," *Journal of Marine Science and Technology*: Vol. 20: Iss. 5, Article 15.

DOI: 10.6119/JMST-012-0814-1

Available at: <https://jmstt.ntou.edu.tw/journal/vol20/iss5/15>

This Research Article is brought to you for free and open access by Journal of Marine Science and Technology. It has been accepted for inclusion in Journal of Marine Science and Technology by an authorized editor of Journal of Marine Science and Technology.

---

# SHALLOW WATER FLOW MODELING USING SPACE-TIME LEAST-SQUARES FINITE-ELEMENT METHOD

## Acknowledgements

The authors would like to thank the National Science Council of Taiwan, the Republic of China, for financial support (Project nos.: NSC 100-2221-E-019-004-MY3 and 100- 2221-E-019-004-MY3).

# SHALLOW WATER FLOW MODELING USING SPACE-TIME LEAST-SQUARES FINITE-ELEMENT METHOD

Shin-Jye Liang, Chiung-Yang Lan, and Ying-Chih Chen

Key words: convection-diffusion equation, shallow-water equations, space-time, least-squares finite-element method.

## ABSTRACT

Various algorithms of least-squares finite-element methods (LSFEM) for convection-diffusion equation (CDE) and shallow-water equations (SWE) are formulated. The associated condition number of the resulting system of equations is systematically compared. It is found that condition number of the resulting system of equations depends on the choice of variables, interpolations, and size of element ( $\Delta x$ ). In general, a better conditioned system is obtained by introducing auxiliary variable with low-order interpolation. The developed better conditioned shallow-water model is used to simulate wave propagation over a submerged bar and wave propagation past an elliptical hump. Computed results are compared with experiment data and other numerical approximation, and show good agreement.

## I. INTRODUCTION

Shallow-water equations (SWE) has wide range applications in ocean, environmental and hydraulic engineering, such as, tidal flows in estuary and coastal regions, and open-channel flows in rivers and reservoirs. SWE is a system of nonlinear hyperbolic conservation laws that admits sharp gradient solutions like shock waves and expansion fans [11, 21]. Numerical solution of SWE has been a challenging task because of its nonlinear nature and the need to satisfy the C-property [16, 17]. The presence of source terms in momentum equations, such as the bottom slope and friction of bed, compounds the difficulties further [1, 8, 14, 19, 20].

Various algorithms of least-squares finite-element method (LSFEM) can be formulated for an ordinary/partial differential

equation, depending on the choice of variables, interpolations, least-squares norm, the least-squares system, and possible including the treatment of boundary conditions [4, 7, 8, 10, 12]. The associated condition number which determines the sensitivity and accuracy of approximations has not well been studied yet. Lan [13] has systematically studied the condition number of the resulting system of equations of 1D convection-diffusion equation (CDE) using various LSFEMs.

LSFEM for SWE using finite-element in space and  $\theta$ -method in time integration has been studied previously [16, 17]. The method is extended using space-time finite-element approach in this study. Condition number of the resulting system of equations of 1D shallow-water equations (SWE) by various LSFEMs is systematically investigated. A better conditioned 2D SWE model by space-time LSFEM is developed and used to study wave-bathymetry interactions, such as wave over a submerged bar [2, 3] and wave past an elliptical hump [1].

The paper is organized as follows. Convection-diffusion equation (CDE) and shallow-water equations (SWE) are introduced first. Formulation of CDE and SWE using least-squares finite-element method is described briefly. Numerical results of CDE and SWE, particularly the condition number of the resulting system of equations, are then presented. Based on the computed results, summaries and conclusions are made.

## II. GOVERNING EQUATIONS

We use 1D convection-diffusion equation (CDE) and shallow-water equations (SWE) to elucidate the formulation of least-squares finite-element method. 1D CDE reads

$$c \frac{\partial u}{\partial x} = d \frac{\partial^2 u}{\partial x^2} \quad (1)$$

where  $u$  is an unknown to be solved, e.g. temperature or concentration,  $c$  and  $d$  denote the convection speed and diffusion coefficient, respectively.

Depth-averaged 1D SWE is derived from equation of 2D mass and momentum conservation based upon assumption of incompressibility of water, hydrostatic pressure, and a suffi-

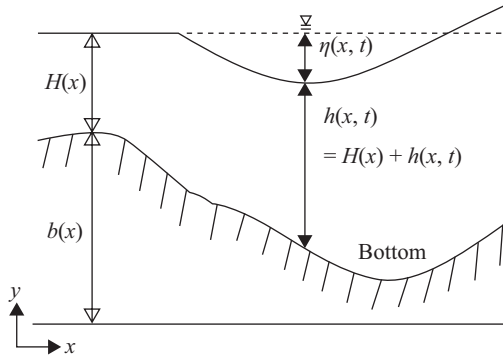


Fig. 1. Illustration of still water depth ( $H$ ), surface ( $\eta$ ), and total water depth ( $h$ ), respectively.

ciently small channel slope [11, 21]. The 1D non-viscous SWE expressed in a non-conservative form reads

$$\begin{cases} \frac{\partial \eta}{\partial t} + \frac{\partial}{\partial x} [(H + \eta)u] = 0 \\ \frac{\partial u}{\partial t} + u \frac{\partial u}{\partial x} + g \frac{\partial \eta}{\partial x} = -g \frac{\partial b}{\partial x} \end{cases} \quad (2)$$

Fig. 1 illustrates symbols used. Where  $\eta$  and  $u$  are the free water surface and velocity,  $b$  is the bottom height,  $H$  is the still water depth,  $g$  is the gravity acceleration,  $x$  denotes the wave travelling direction,  $t$  is the time, respectively.

### III. SPACE-TIME LEAST-SQUARES FINITE-ELEMENT FORMULATIONS

We use steady 1D CDE to illustrate the formulation of least-squares finite-element methods (LSFEM), and then extend the method for unsteady 1D SWE by space-time LSFEM.

#### 1. Convection-Diffusion Equation

By introducing an auxiliary variable, i.e.  $w = \partial u / \partial x$ , to reduce the order of the equation, CDE can be rewritten as

$$\begin{cases} c \frac{\partial u}{\partial x} = d \frac{\partial w}{\partial x} \\ w = \frac{\partial u}{\partial x} \end{cases} \quad (3)$$

In finite-element method, the unknowns ( $\underline{u} = \{u, w\}^T$ ) are approximated by polynomial interpolations, and substituted into differential equation to find the residuals, i.e.  $R$ . The least-squares functional and its minimization principle are then constructed

$$\text{minimize } \int_{\Omega} R^2 d\Omega \quad (4)$$

where  $\Omega$  is the space domain considered. The above equation is equivalent to

$$\int_{\Omega} \left\{ \frac{\partial R}{\partial \underline{u}} \right\}^T R d\Omega = 0 \quad (5)$$

Various algorithms can be formulated, depending on the choice of variables, interpolations, least-squares norm, and possible including the treatment of boundary conditions [7, 10]. Formulations are categorized into two kinds: (a) direct approach (so called  $U$ -formulation) where quadratic interpolation function are used, and (b) order-reducing approach (so called  $UW$ -formulation) where an auxiliary variable is introduced to reduce the order of differential equation, such that linear interpolation function can be used. Therefore, three formulations, including (a)  $U$ -Quadratic, (b)  $UW$ -Linear, and (c)  $UW$ -Quadratic, formulation are considered. In (a)  $U$ -Quadratic formulation, unknown  $u$  is approximated by a quadratic interpolation, and least-squares minimization can be applied directly. In (b)  $UW$ -Linear and (c)  $UW$ -Quadratic formulation, unknown  $u$  and  $w$  are approximated by linear or quadratic interpolations, respectively. Least-squares minimization is then applied. Details of the LSFEM formulation are referred to [4, 6, 7, 10].

#### 2. Shallow-Water Equations

We use 1D non-viscous SWE, Eq. (2), to illustrate the formulation of space-time LSFEM. Eq. (2) is first linearized by Newton's method

$$\begin{cases} \frac{\partial \eta}{\partial t} + H \frac{\partial u}{\partial x} + u \frac{\partial d}{\partial x} + \frac{\partial}{\partial x} (\tilde{\eta}u + \eta\tilde{u} - \tilde{\eta}\tilde{u}) = 0 \\ \frac{\partial u}{\partial t} + \left( \tilde{u} \frac{\partial u}{\partial x} + u \frac{\partial \tilde{u}}{\partial x} - \tilde{u} \frac{\partial \tilde{u}}{\partial x} \right) + g \frac{\partial \eta}{\partial x} = -g \frac{\partial b}{\partial x} \end{cases} \quad (6)$$

where “ $\sim$ ” represents value from previous iteration or time step.

In finite-element method, the unknowns ( $\underline{u} = \{\eta, u\}^T$ ) are approximated by polynomial interpolations

$$\begin{Bmatrix} \eta(x, t) \\ u(x, t) \end{Bmatrix} = \begin{bmatrix} M(x)N(t) \\ M(x)N(t) \end{bmatrix} \begin{Bmatrix} \eta \\ u \end{Bmatrix} \quad (7)$$

where  $M(x)$  and  $N(t)$  are space and time interpolation function, respectively. Substituted approximations, Eq. (7), into Eq. (6), residuals can be obtained

$$\begin{Bmatrix} R_{\eta}^e \\ R_u^e \end{Bmatrix} = \begin{bmatrix} \tilde{u}_x MN_1 + MN_1' + \tilde{u}M'N_1 & (\tilde{\eta}_x + H)MN_1 + (H + \tilde{\eta})M'N_1 \\ gM'N_1 & \tilde{u}_x MN_1 + MN_1' + \tilde{u}M'N_1 \end{bmatrix} \begin{Bmatrix} \eta \\ u \end{Bmatrix}^n + \begin{bmatrix} \tilde{u}_x MN_2 + MN_2' + \tilde{u}M'N_2 & (\tilde{\eta}_x + H)MN_2 + (H + \tilde{\eta})M'N_2 \\ gM'N_2 & \tilde{u}_x MN_2 + MN_2' + \tilde{u}M'N_2 \end{bmatrix} \begin{Bmatrix} \eta \\ u \end{Bmatrix}^{n+1} \quad (8)$$

**Table 1. Comparison of condition number of different least-squares formulations of CDE.**

	dofs	$E = 10$	$E = 20$	$E = 40$	$E = 1,000$
U-Quadratic Formulation	$2E + 1$	cond(A) = 3.0671e+08	cond(A) = 1.9847e+10	cond(A) = 1.2737e+12	cond(A) = 9.7135e+17
UW-Linear Formulation	$2E + 2$	cond(A) = 1.1265e+03	cond(A) = 4.3736e+03	cond(A) = 1.7150e+04	cond(A) = 1.0483e+07
UW-Quadratic Formulation	$4E + 2$	cond(A) = 5.8237e+03	cond(A) = 2.2859e+04	cond(A) = 9.0439e+04	cond(A) = 5.5879e+07
Central Difference	$E + 1$	cond(A) = 40.1545	cond(A) = 159.4800	cond(A) = 638.2332	cond(A) = 3.9914e+05
1 <sup>st</sup> -order upwind Difference	$E + 1$	cond(A) = 40.2850	cond(A) = 159.6137	cond(A) = 638.4730	cond(A) = 3.9915e+05

Note: Condition number of system of equations  $Ax = b$  is computed using Matlab cond function, i.e. cond(A).  $E$  denotes number of elements.

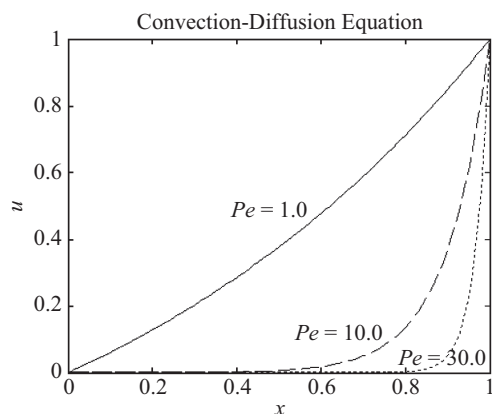


**Fig. 2. Exact solution of convection-diffusion equation for  $Pe = 1, 10$  and  $30$ , respectively.**

Note that piecewise linear interpolation function for time is used, where subscripts “1” and “2” denotes number of local node, superscripts “ $n$ ” and “ $n+1$ ” denote value of the space-time element at  $t = t^n$  and  $t^{n+1}$ , respectively. The least-squares functional and its minimization principle are then constructed, same as Eqs. (4) and (5). Details of the space-time finite-element formulation can be found in [9, 18].

#### IV. NUMERICAL RESULTS

Three cases, including condition number study of CDE and SWE, wave over a submerged bar [2], and wave past an elliptical hump [1] are studied.

##### 1. Condition Number Study of Convection-Diffusion Equation and Shallow-Water Equations

We use 1D CDE as a test problem to examine the performance of each LSFEM algorithm. The exact solution corresponding to Eq. (1) with boundary condition  $u(0) = 0$  and  $u(1) = 1$  is

$$u(x) = \frac{1 - e^{-Pe \cdot x}}{1 - e^{-Pe}} \quad (9)$$

where Peclet number  $Pe = cL/d$ . Fig. 2 depicts the exact solution of CDE for  $Pe = 1, 10$  and  $30$ , respectively. Note boundary layer type solution near the right boundary develops

as  $Pe$  increases.

For U-Quadratic algorithm, without introducing auxiliary variable and using a quadratic element, each element contains three nodes and each node has one variable ( $u$ ), total three degree-of-freedom (dofs); For UW-Linear algorithm, with introducing auxiliary variable ( $w$ ) and using a linear element, each element contains two nodes and each node has two variables ( $u$  &  $w$ ), total four dofs; For UW-Quadratic algorithm, with introducing auxiliary variable ( $w$ ) and using a quadratic element, each element contains three nodes and each node has two variables ( $u$  &  $w$ ), total six dofs.

Condition number which relates to eigen values of the resulting system of equations, and determines the sensitivity and roundoff error of approximation is used as an indicator to evaluate the numerical performance of the algorithms. Table 1 summaries the comparison of condition number of least-squares algorithms for CDE with (a) U-Quadratic, (b) UW-Linear, (c) UW-Quadratic, (d) central finite-difference, and (e) 1<sup>st</sup>-order upwind finite-difference, respectively. It is evident that condition number increases as element refined ( $\Delta x$  decreases), in particularly for U-Quadratic formation. Order-reduced (UW) formations, i.e. UW-Linear and UW-Quadratic formation, are better conditioned, and therefore, are recommended. Due to least-squares functional, least-squares formulations have larger condition number compared with the counterpart of the finite-difference method with the same computational mesh resolution.

Study of condition number of STLSFEM for 1D SWE with (a) U-Linear, (b) U-Quadratic, (c) UW-Linear, and (d) UW-Quadratic formulation is also performed. Table 2 summarizes comparison of condition number resulting from simulating a sinusoidal wave propagating in a flat channel [5]. It is found high-order approximations result in a larger system of equations and larger condition number. Condition number increases proportionally to  $\Delta x^{-1.5}$  for both U- and UW-Linear formation, and proportionally to  $\Delta x^{-2}$  for both U- and UW-Quadratic formation, as element refined. Moreover, UW-formulation results in much larger condition number of resulting system of equations than U-formulation does, and may cause large roundoff error.

##### 2. Wave over A Submerged Bar

A regular wave propagating over a submerged bar, similar to wave flume experiment of Beji and Battjes [2], see Fig. 3, is

**Table 2. Comparison of condition number of different least-squares formulations of SWE.**

	dofs	$E = 80$	$E = 160$	$E = 320$	$E = 640$
U-Linear Formulation	$2E + 2$	cond(A) = 656.2181	cond(A) = 770.9381	cond(A) = 2.2173e+003	cond(A) = 7.5017e+003
U-QuadraticFormulation	$4E + 2$	cond(A) = 1.2525e+003	cond(A) = 4.6389e+003	cond(A) = 2.0015e+004	cond(A) = 9.0375e+004
UW-Linear Formulation	$3E + 3$	cond(A) = 1.8766e+006	cond(A) = 4.4930e+006	cond(A) = 1.3214e+007	cond(A) = 5.5787e+007
UW-QuadraticFormulation	$6E + 3$	cond(A) = 6.4515e+006	cond(A) = 2.4278e+007	cond(A) = 1.5914e+008	cond(A) = 1.6737e+009

Note: Condition number of system of equations  $Ax = b$  is computed using Matlab cond function, i.e. cond(A).  $E$  denotes number of elements.

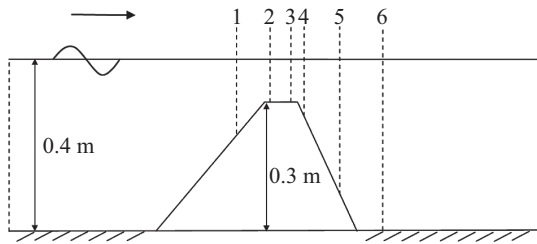


**Fig. 3. Wave past a submerged bar: Schematic of experiment of Beji and Battjes [2].**

simulated by SWE model to study the bathymetry effect on wave deformation [5]. In the experiment a wave flume with length  $L_0 = 25$  m, an incident wave with period  $T = 2$  s and wave amplitude  $a = 0.01$  m is specified at left boundary and radiates out the right boundary. The still water depth is  $H = 0.4$  m, and shoals to 0.1 m over the bar, i.e.  $kH$  ( $k$  is the wave number) ranges from 0.68 to 0.32. The submerged bar has a 1:20 slope and a 1:10 slope frontward and backward, respectively.  $\Delta x = 1/30$  m and  $\Delta t = 0.0005$  s is used in computations. Six wave gauges are selected, see Fig. 3 and Table 3, where time history of water surface is recorded.

Comparison of time history of water surface between SWE modeling and experiment data is depicted in Fig. 4. Wave deforms on the upslope due to the decrease of water depth. Good agreement in term of wave height and phase speed at station 1 and 2, Fig. 4 (a) and (b), is found. However, wave deforms on the downward slope is not accurately predicted, as illustrated in 3 (c)-(e). High harmonics are generated and observed.

Fig. 5 shows the comparison of the power spectrum analysis of time history of surface elevation between computed results and corresponding experiment data. High harmonics increase gradually through the upslope as nonlinear effect becomes significant, as illustrated at stations 1 and 2. Experimental spectra shows that all components become free and the energy of the second harmonic is higher than the first one over the bar crest, i.e. at stations 3-6. SWE model cannot reproduce these high harmonics. This discrepancy is attributed to the non-dispersion assumption of SWE model. To accurately reproduce this experiment data, the dispersion term should be included, such as Boussinesq equations model [3, 15].

### 3. Wave Past an Elliptical Hump

Finite-element method is based on the unstructured meshes

**Table 3. Location of wave gauges of experiment of Beji and Battjes [2].**

Gauge	1	2	3	4	5	6
$x$ (m)	10.8	12.8	13.8	14.8	16	17.6

computations. Extension of the method to 2D is straightforward [16, 17]. Application of the model for flow past an elliptical hump [1, 10] is investigated. The bottom topography is shown in Fig. 6 and given by

$$z(x, y) = 0.8 \exp(-5(x - 0.9)^2 - 50(y - 0.5)^2) \quad (10)$$

We consider the initial condition with water surface perturbed by the upward displacement 0.01 m in the region  $0.05 \leq x \leq 0.15$

$$\eta(x, y, 0) = \begin{cases} 0.01 \text{ m} & \text{if } 0.05 \leq x \leq 0.15 \\ 0 \text{ m} & \text{otherwise} \end{cases} \quad (11)$$

The initial momentum in the  $x$  and  $y$  direction is zero

$$u(x, y, 0) = v(x, y, 0) = 0 \text{ m/s} \quad (12)$$

The computational domain is  $[0, 2] \times [0, 1]$ . After performing refinement of mesh resolution and time increment,  $\Delta x = \Delta y = 0.01$  m (a  $200 \times 100$  uniform 9-node quadrilateral elements) and  $\Delta t = 0.001$  s are used for computations.

Fig. 7 shows comparison of computed water surface of the present study with the numerical result of Liang and Hsu [16] ( $\Delta x = \Delta y = 0.01$  m, and  $\Delta t = 0.0005$  s) and Akoh, *et al.* [1] ( $\Delta x = \Delta y = 0.01$  m, and  $\Delta t = 0.0005$  s). It shows a 30 uniformly spaced 2D contour lines of water surface level ( $\eta$ ) at various time instances. The initial perturbation propagates and exits the left boundary with unnoticeable reflection; It propagates to right and is affected by the bottom. Shoaling effect (increasing the amplitude of wave due to the decreasing of water depth) is obvious at  $t = 0.24$  s. The wave speed is slower above the hump (due to the shallow water depth) than elsewhere, leading to a distortion of the initially planar perturbation. Reflections and interactions of the surface waves result in complex and symmetrical wave structures. Standing waves due to the reflection of the hump behind the wave tail is observed at

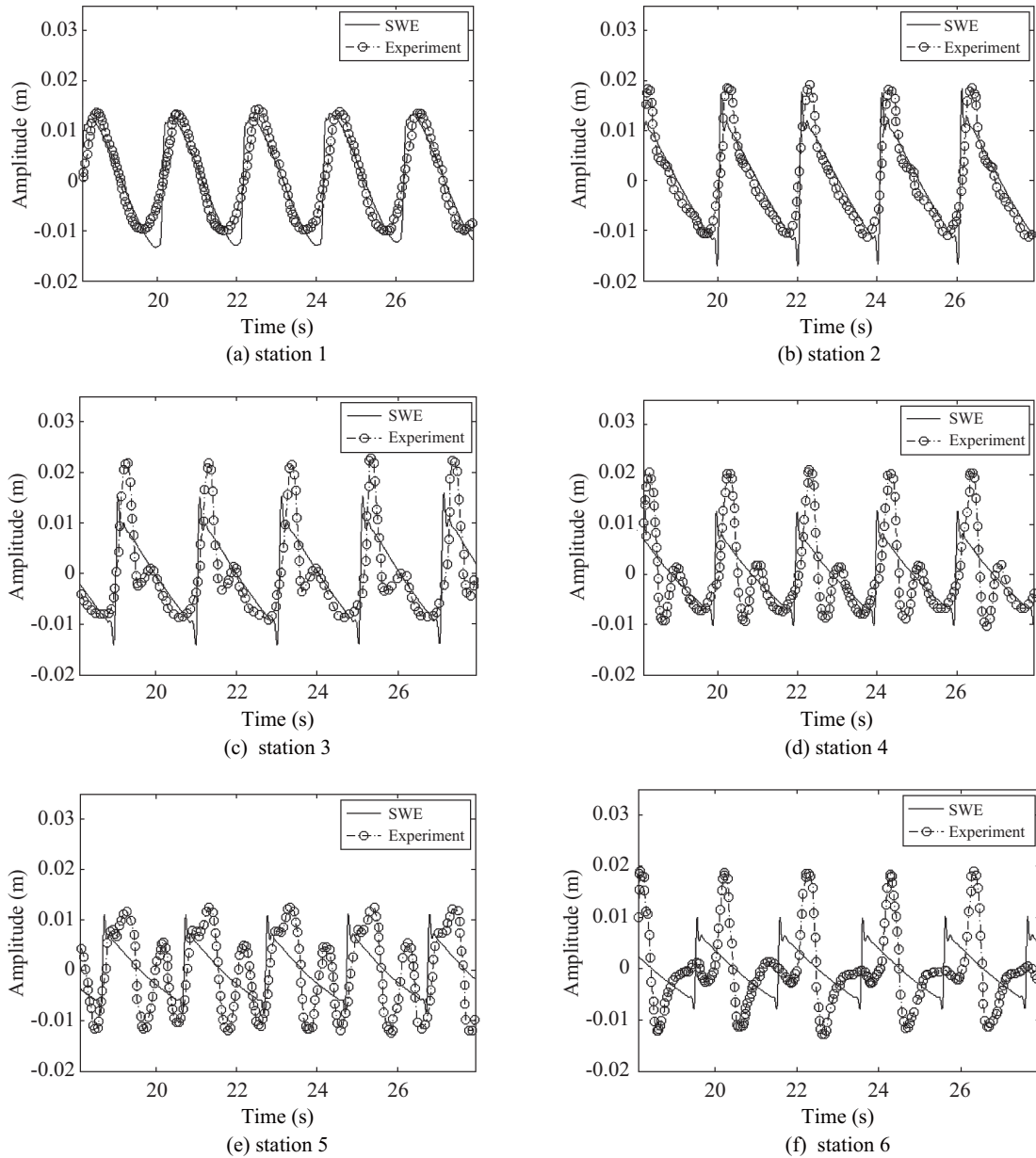


Fig. 4. Wave over a submerged bar: Comparison of time history of free surface at stations 1-6. Numerical results (—) and experimental data (---○---).

$t = 0.24, 0.36, 0.48,$  and  $0.6$  s, respectively. These fine detailed wave structures were not observed in Liang and Hsu [16], Akoh, *et al.* [1], and LeVeque [10]. The present model which employs a quadratic approximation is apparently better to resolve the symmetrical and fine structures. Overall, predictions of the present model give sharper gradients and more detailed wave structures than the numerical results of Liang and Hsu [16], Akoh, *et al.* [1], and LeVeque [10].

## V. CONCLUSION

Different algorithm based on the least-squares finite-element method can be formulated depending on the choice of

variables, interpolations, least-squares norm, the least-squares system, and possible including the treatment of boundary conditions. Based on the computed results of convection-diffusion equation and shallow-water equations, the following conclusions can be made:

1. Combining reduced-order approach (UW-formulation) with low-order interpolations results in a better conditioned system of equations, and therefore, is more stable and accurate, as illustrated in Table 1 for CDE. However, the methods may result in more dofs, i.e. a larger system of equations to be solved.
2. High-order approaches are suitable for resolving large

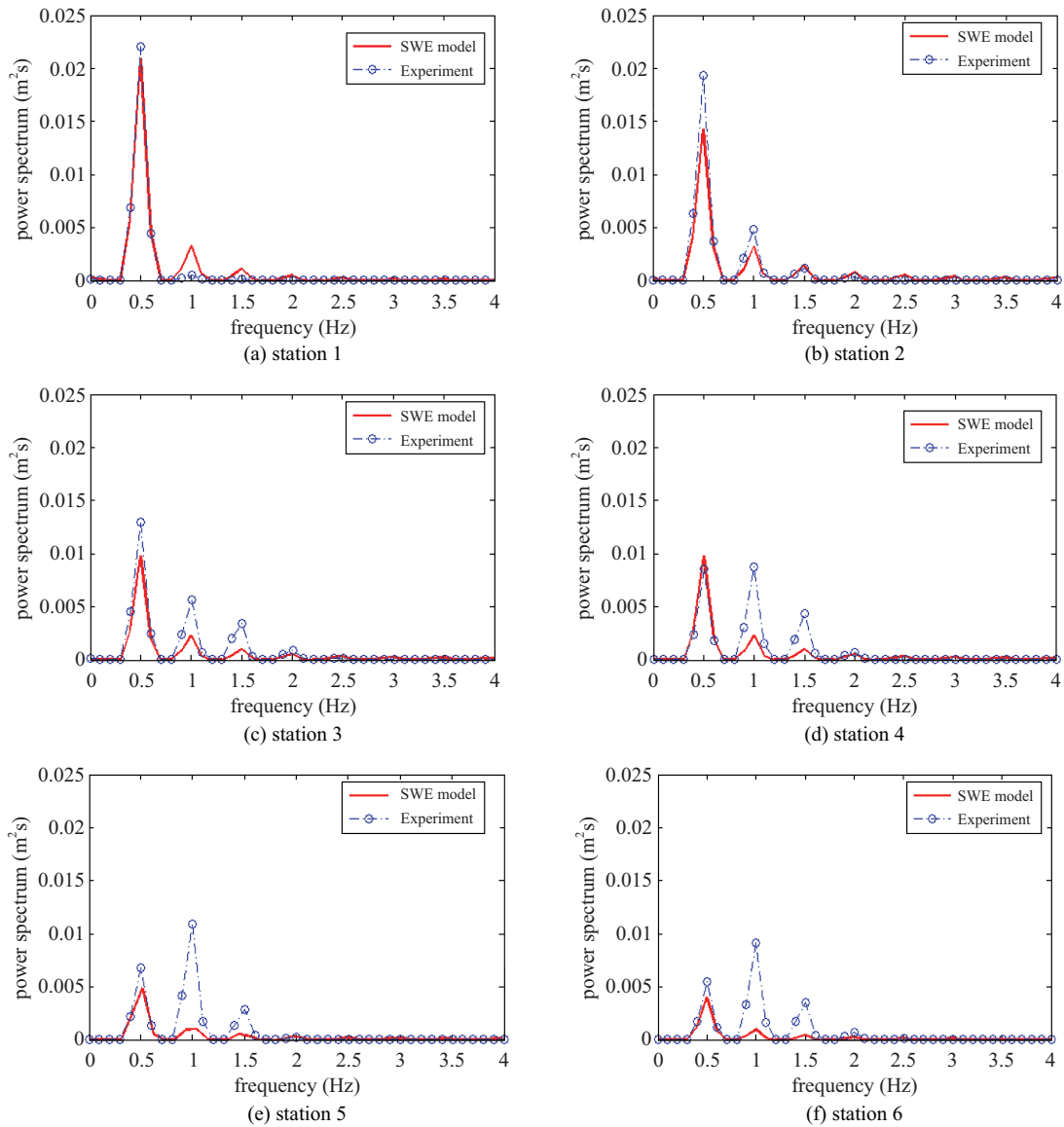


Fig. 5. Wave over a submerged bar: Comparison of spectrum density of surface elevation at stations 1~6. Numerical results (—) and experimental data (---○---).

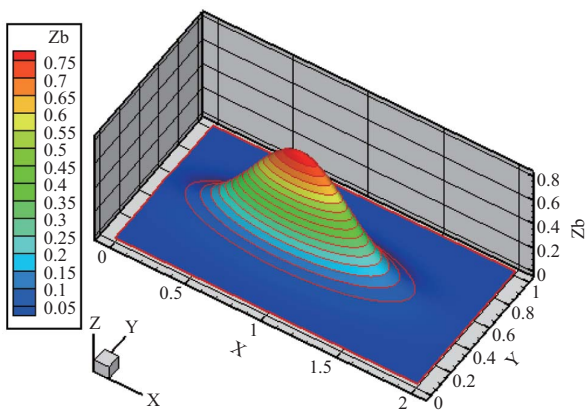


Fig. 6. Flow past an elliptical hump: Illustration of the computational domain and the elliptical shaped hump.

gradients and fine structure of flow/wave fields. They usually result in more dofs and a poor conditioned system of equations. There are trade-offs and compromises for the reduced-order approaches and high-order interpolations. Combination of the two approaches, UW-formulation with high-order interpolations, provide a poor conditioned algorithm, and may introduce large roundoff error of approximations, as illustrated in Table 2 for SWE, in general.

Space-time finite-element method is particularly suitable for differential equations containing spatial and temporal mixed derivative terms, such as the dispersion terms in Boussinesq equations. Preliminary results of application of space-time LSFEM for Boussinesq equations is promising, and will be published in a separated paper.

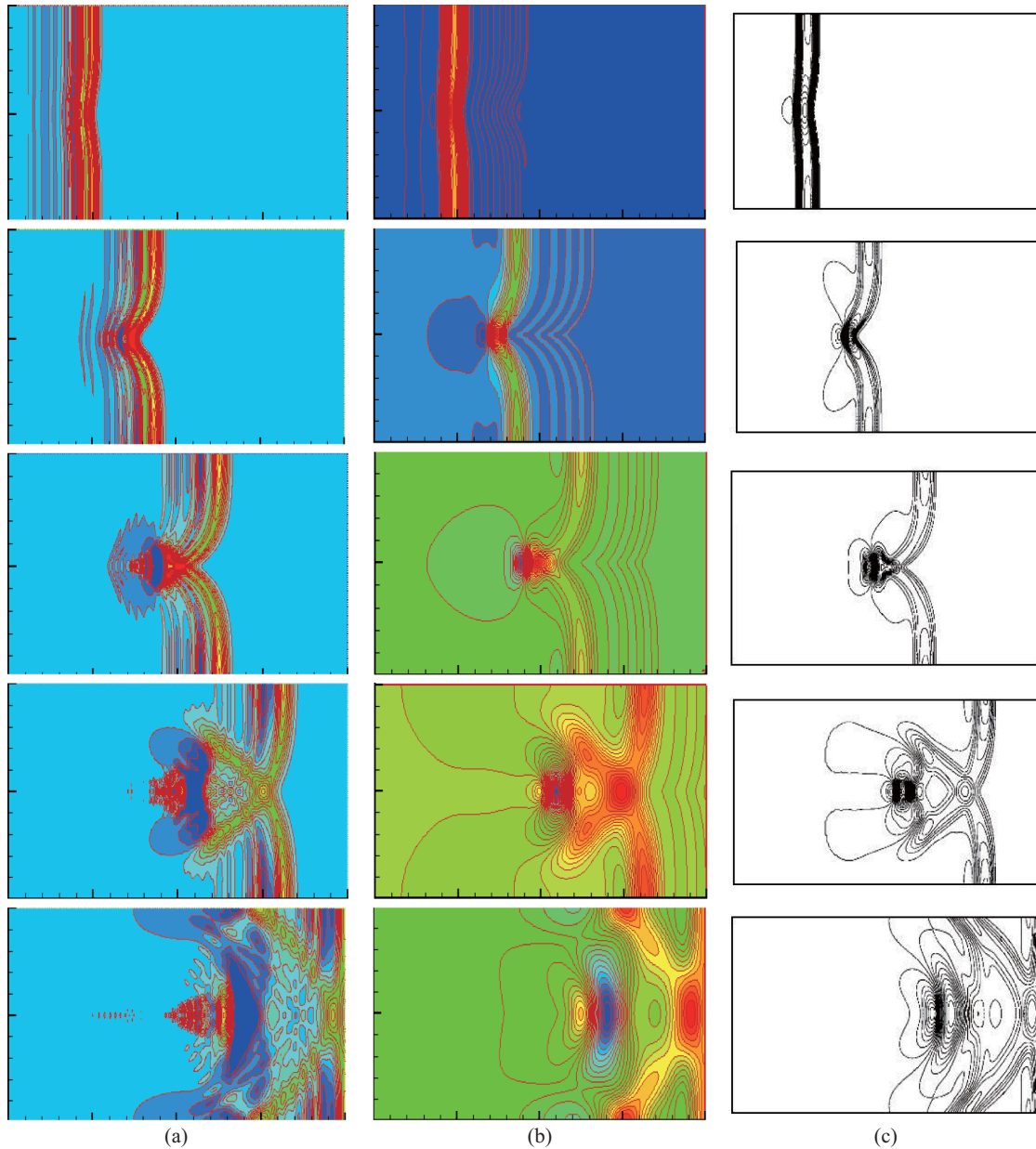


Fig. 7. Wave past an elliptical hump: 2D contours of the water surface of (a) present study with 9-node quadrilateral elements (left), and (b) results of Liang and Hsu [16] with 3-node triangular meshes (middle), and (c) result of Akoh, *et al.* [1] (right) at  $t = 0.12, 0.24, 0.36, 0.48,$  and  $0.6$  s, respectively.

## ACKNOWLEDGMENTS

The authors would like to thank the National Science Council of Taiwan, the Republic of China, for financial support (Project nos.: NSC 100-2221-E-019-004-MY3 and 100-2221-E-019-004-MY3).

## REFERENCES

1. Akoh, R., Li, S., and Xiao, F., "A CIP/multi-moment finite volume method for shallow water equations with source terms," *International Journal for Numerical Methods in Fluids*, Vol. 56, pp. 2245-2270 (2008).
2. Beji, S. and Battjes, J. A., "Experimental investigation of wave propagation over a bar," *Coastal Engineering*, Vol. 19, pp. 151-162 (1993).
3. Beji, S. and Battjes, J. A., "Numerical simulation of nonlinear wave propagation over a bar," *Coastal Engineering*, Vol. 23, pp. 1-16 (1994).
4. Bochev, P. B. and Gunzburger, M. D., "Finite element methods of least-squares type," *SIAM Review*, Vol. 40, pp. 789-837 (1998).
5. Chen, Y.-C., *Comparison of Numerical Solution of Shallow-Water Equations and Boussinesq Equations for Wave Propagation over a Submerged Bar*, Master Thesis, Department of Marine Environmental Informatics, National Taiwan Ocean University, Taiwan (2012).
6. Deang, J. M. and Gunzburger, M. D., "Issues related to least-squares finite element methods for the Stokes equations," *SIAM Journal on Scientific Computing*, Vol. 20, pp. 878-906 (1998).
7. Gunzburger, M. D., *Finite Element Methods for Viscous Incompressible Flows*, Academic Press (1989).

8. Hervouet, J.-M., *Hydrodynamics of Free Surface Flows: Modelling with the Finite Element Method*, John Wiley & Sons (2007).
9. Hughes, T. J. R. and Hulbert, G. M., "Space-time finite element methods for elastodynamics: formulations and error estimates," *Computer Methods in Applied Mechanics and Engineering*, Vol. 66, pp. 339-363 (1988).
10. Jiang, B. N., *The Least-Squares Finite Element Method*, Springer (1998).
11. Johnson, R. S., *A Modern Introduction to the Mathematical Theory of Water Waves*, Cambridge (1997).
12. Laibel, J. P. and Pinder, G. F., "Solution of the shallow water equations by least squares collocation," *Water Resources Research*, Vol. 29, pp. 445-455 (1993).
13. Lan, C.-Y., *Application of Adaptive Binary Mesh Based on Space-Time Least-Squares Finite Element Method*, Master Thesis, Department of Marine Environmental Informatics, National Taiwan Ocean University, Taiwan (2012).
14. LeVeque, R. J., "Balancing source terms and flux gradients in high-resolution Godunov methods: The quasi-steady wave-propagation algorithm," *Journal of Computational Physics*, Vol. 146, pp. 346-365 (1998).
15. Li, Y. S. and Zhan, J. M., "Boussinesq-type model with boundary-fitted coordinate system," *Journal of Waterway, Port, Coastal, and Ocean Engineering*, Vol. 127, pp. 152-160 (2001).
16. Liang, S.-J. and Hsu, T.-W., "Least-squares finite-element method for shallow-water equations with source terms," *Acta Mechanica Sinica*, Vol. 25, pp. 523-532 (2009).
17. Liang, S.-J., Tang, J.-H., and Wu, M.-S., "Solution of shallow-water equations using least-squares finite-element method," *Acta Mechanica Sinica*, Vol. 24, pp. 523-532 (2008).
18. Tezduyar, T. E., Behr, M., Mittal, S., and Liou, J., "A new strategy for finite element computations involving moving boundaries and interfaces – The deforming-spatial-domain/space-time procedure: II. Computation of free-surface flows, two-liquid flows, and flows with drifting cylinders," *Computer Methods in Applied Mechanics and Engineering*, Vol. 94, pp. 353-371 (1992).
19. Toro, E. F., *Riemann Solvers and Numerical Methods for Fluid Dynamics*, Springer-Verlag (1997).
20. Toro, E. F., *Shock-Capturing Methods for Free-Surface Shallow Flows*, John Wiley & Sons (2001).
21. Whitham, G. B., *Linear and Nonlinear Waves*, Wiley-Interscience (1999).